



Mass spectrometry-based characterization of acidic glycans on protein therapeutics

Paul A. Salinas, May Joy C. Miller, Melanie X. Lin, Phil J. Savickas, John J. Thomas*

Shire Human Genetic Therapies, Pharmaceutical and Analytical Development, 700 Main St., Cambridge, MA 02139, USA

ARTICLE INFO

Article history:

Received 1 April 2011

Received in revised form 22 June 2011

Accepted 23 June 2011

Available online 30 June 2011

Keywords:

Glycoprotein

Therapeutics

N-linked glycan

Phosphorylation

Sulfonation

ABSTRACT

Glycosylation is a critical posttranslational modification that affects the physiochemical and biological properties of glycoproteins. Specifically, acidic glycans such as phosphorylated, sialylated and sulfonated glycoforms have well known biological implications; therefore, a detailed understanding of these structures is essential for defining the attributes of therapeutic glycoproteins. The clinical significance of these attributes has increased the analytical requirements for development of therapeutic glycoproteins. Despite current advances in mass-spectrometric methodologies, challenges remain in characterizing these heterogeneous modifications. Here we present the global and site-specific characterization of acidic N-linked glycans from three therapeutic enzymes, velaglucerase alfa, idursulfase and agalsidase alfa. Orthogonal methodologies, including MALDI-TOF MS, static ESI-MS/MS, RPLC-MS, and HILIC-MS, are used to characterize N-linked glycans to support the development of enzyme replacement therapeutics. In addition, the results of these studies can provide identification, structural elucidation, and quantitation of the different acidic glycoforms that is often used to understand the glycan composition of these molecules during product development.

© 2011 Elsevier B.V. All rights reserved.

1. Introduction

The glycan composition of therapeutic glycoproteins potentially can contribute to their safety, efficacy, and stability [1–3]. Glycosylation is often a critical posttranslational modification that defines a therapeutic glycoprotein's intrinsic properties, such as its biological activity, solubility, and pharmacokinetics [4–6]. Specifically, acidic glycans containing sialic acid, phosphate, or sulfate have well-documented structural properties with specific functional roles in biological processes involving cellular uptake, elimination, and immunogenicity [5–7]. Asialo complex glycans, for example, are known to have reduced circulatory half-lives compared to their fully sialylated counterparts, while N-glycolylneuraminic acid has been implicated in human immunogenic responses [5–7]. Other functional roles include the efficient cellular uptake of lysosomal enzymes as mediated by N-glycans with mannose-6-phosphate [8,9] or the potential for enhanced circulatory clearance of sulfonated N-linked glycans [10,11]. Therefore, the presence or absence of acidic glycans is often the basis for determining the critical quality attributes of therapeutic glycoproteins and requires characterization and control from early product development through licensure and beyond.

An early understanding of glycosylation patterns can benefit various aspects of therapeutic development: in cell culture process development where media growth conditions can affect glycosylation patterns, in purification development where chromatography can be affected by known glycosylation attributes, and during development of analytical characterization and testing methods where glycan microheterogeneity can affect assay results. Additionally, robust glycan characterization techniques are especially important for establishing process controls that aid in production of comparable product batches. The importance of these assays becomes even greater when developing biosimilars.

Analytical methods commonly used to analyze N-linked glycans, such as monosaccharide analysis and high-performance anion-exchange chromatography with pulsed amperometric detection (HPAEC-PAD), allow for quantitative comparison of particular carbohydrates but do not provide detailed compositional or structural information. The evolution of mass spectrometric-based methods has provided tools for the structural characterization of glycans that can assess a variety of glycan features.

Here we will discuss two mass spectrometric-based approaches that aid in the characterization of N-linked glycans found on therapeutic glycoproteins: global structural characterization and site-specific compositional approaches. The global characterization approach monitors changes in the entire glycan pool, either through analysis of the intact glycoprotein, or through analysis of the released glycans, which can provide detailed linkage information. Site-specific compositional analysis, on the other hand, can

* Corresponding author. Tel.: +1 617 613 4402.

E-mail address: jthomas@shire.com (J.J. Thomas).

provide a means of identifying the glycan types found at each of the individual sites of glycosylation.

Previous reports show that phosphorylated glycans can mediate the cellular trafficking of lysosomal enzymes via the mannose-6-phosphate receptor and the structure of these glycans can have a significant impact on receptor targeting and uptake kinetics for these enzymes [12,13]. The characterization of these types of glycan structures has previously been performed through certain biochemical and bioanalytical methods. Receptor binding and cellular internalization, for example, were assessed using *in vitro* and *in vivo* systems by removal of phosphorylated glycans or mannan-6-phosphate inhibition [6,14,15]. In the work presented here, several mass spectrometric methodologies were utilized to identify and elucidate the structures of phosphorylated high-mannose glycans on velaglucerase alfa and agalsidase alfa enzymes to support the development of enzyme replacement therapies for Gaucher and Fabry patients.

In addition to phosphate, we identify another posttranslational modification, sulfonation that contributes an additional mass of 80 Da to the complex glycans of the therapeutic lysosomal enzyme idursulfase used to treat Hunter patients. While phosphorylation and sulfonation add the same nominal mass, the physiochemical properties of phosphate and sulfate are distinctly different and thus require additional characterization methods presented here.

2. Experimental

For the described experiments, the therapeutic glycoproteins velaglucerase alfa, agalsidase alfa, and idursulfase came from Shire Human Genetic Therapies (Cambridge, MA).

2.1. Global structural characterization of glycans: intact protein analysis

The charge characteristics of many proteins, including the above glycoproteins, are often defined by their ion-exchange chromatographic profiles. The charge variants of intact velaglucerase alfa are quantitatively tested by an ion-exchange high-performance liquid chromatography (IEX-HPLC) method using a weak cation-exchange column (ProPac WCX-10, 4 mm × 250 mm, Dionex, Corp.). Individual peak fractions were collected from the WCX column, concentrated using a centrifugal concentration device (Micron 10 kDa MW filter, Millipore, Corp.), and analyzed by reversed-phase liquid chromatography with mass-spectrometric detection (LC-MS). LC-MS analysis utilized a Tempo nano LC (Eksigent) coupled to a QSTAR Elite™ quadrupole time-of-flight mass spectrometer (Applied Biosystems/ABSciex). The analysis utilized the two-dimensional (2D) chromatography capabilities of the nano LC system, which was equipped with an on-line C₁₈ trap column (Captrap C18, Michrom International, GmbH) and a C₁₈ analytical column (1 mm × 150 mm ID, ACE®). Glycoproteins were eluted with a linear gradient from 38 to 58% acetonitrile, 2% formic acid, 0.03% heptafluorobutyric acid (HFBA) at a 5 µL/min flow rate.

Mass accuracy of approximately 20 ppm was achieved for intact velaglucerase alfa using angiotensin (Sigma–Aldrich, Corp.) for external calibration prior to LC-MS analysis. Deconvolution of the multiply-charged species was performed with the instrument manufacturer's Bayesian protein reconstruct algorithm, which occurred after Gaussian smoothing and baseline subtraction of the raw mass spectra.

2.2. Global structural characterization of glycans: total glycan release

Permethylation of the PNGase F released glycans of velaglucerase alfa and agalsidase alfa were prepared accord-

ing to the method described by Ciucanu and Kerek [16]. Dried glycans were reconstituted with a DMSO/NaOH suspension, vortexed and allowed to react at room temperature with occasional vortexing. Methyl iodide (CH₃I, Sigma–Aldrich, Corp.) was added to this solution, and allowed to react at room temperature. The permethylated glycans were extracted with chloroform, dried under a stream of nitrogen, and further purified by solid phase extraction.

Permethylated glycans were desalted using a C₁₈ ZipTip (Millipore, Corp.) with a wash solution of 0.1% trifluoroacetic acid (TFA) in water and were eluted with 50% acetonitrile, 0.1% TFA. For MALDI-TOF MS analysis, the sample was mixed 1:1 with matrix (2,5-dihydroxybenzoic acid, Waters, Corp.) and 0.5 µL of 20 mM sodium acetate. Samples were analyzed by MALDI-TOF MS in the positive-ion linear mode using a Voyager-DE Biospectrometry workstation (Applied Biosystems/ABSciex) and in the positive-ion reflectron mode using a Microflex system (Bruker Daltonics, Inc.). ESI-MS spectra were acquired in the positive-ion mode using the QSTAR Elite™ with a Nanospray II ion source (Applied Biosystems/ABSciex). The permethylated glycans were introduced into the mass spectrometer using a spray solution of 50% methanol and an ionization potential of 1400 V. ESI-MS/MS spectra were obtained using a range of collision energies between 55 and 65 eV.

2.3. Site-specific glycan composition analysis

Velaglucerase alfa and idursulfase were prepared for site-specific characterization by enzymatic digestion using reductive denaturation with DTT, followed by cysteine alkylation with iodoacetic acid. Alkylated samples were digested first with endoproteinase Lys-C (Roche Diagnostics, GmbH) using a 1:42 enzyme to substrate ratio (w/w) at 37 °C. Idursulfase required a subsequent treatment with the endoproteinase Glu-C (Roche Diagnostics, GmbH) using a 1:25 enzyme to substrate ratio (w/w) at room temperature to separate closely spaced glycosylation sites. Digested samples were analyzed by peptide mass mapping using reversed-phase chromatography (C₁₈, 2.1 mm × 250 mm, 300 Å column, Phenomenex, Inc.) with a mobile phase system consisting of water, 0.1% TFA and acetonitrile, 0.085% TFA, flowing at a rate of 0.25 mL/min. Detection was performed with an in-line UV (214 nm) detector (model 2684, Waters, Corp.) followed by a 4000 Qtrap (Applied Biosystems/ABSciex) or LTQ-Finnigan (Thermo Scientific) mass spectrometer (LC-UV-MS). Identification of N-linked glycosylation sites was accomplished by comparing the peptide maps before and after glycan release with PNGase F (New England Biolabs, Inc.). Glycan masses were determined by subtracting the expected peptide mass from the observed glycopeptide masses. GlycoMod software from the ExPASy web site (<http://us.expasy.org/tools/glycomod/>) [17] was used to determine potential glycan compositions from the observed masses. To verify the presence of sialic acid, phosphate, or alpha-linked mannose for each of the observed glycan compositions, LC-MS analysis was performed on glycoprotein digests after treatment (according to manufacturer's recommendations) with neuraminidase (Roche Diagnostics, GmbH), alkaline phosphatase (Roche Diagnostics, GmbH), or α-mannosidase (Glyko, Inc.), respectively. To further characterize the sites of glycan phosphorylation and sialylation, LC-MS/MS fragmentation analysis was performed on the glycopeptides.

2.4. Characterization of sulfonated glycans

Enrichment of the sulfonated glycoforms from idursulfase was achieved through strong anion-exchange (SAX) chromatography. The formulated glycoprotein drug product was loaded onto a Q-sepharose column pre-equilibrated with 20 mM tris, pH 7.0. SAX fractions were collected from the column by gradient elution with

20 mM tris, 1 M NaCl (pH 7.0), concentrated and buffer-exchanged for proteolytic digestion. The glycoprotein samples were reduced and carboxymethylated, desalted, and digested through a combination of treatments using endoproteinases Lys-C and Glu-C as previously described. LC–MS analysis of the sulfonated glycopeptides was performed using a LTQ-XL linear ion-trap mass spectrometer (Thermo Scientific).

Sulfonated glycopeptides were separated and collected by reversed-phase chromatography as described above for site-specific characterization. Sulfonated glycopeptides were prepared for enzymatic glycan release by removal of the HPLC organic solvent through evaporative centrifugation and reconstitution of the samples with 50 mM ammonium bicarbonate (pH 7.8). Preparation of released glycans was by incubation with PNGase F at 37 °C and purified from the peptides using C₁₈ solid-phase extraction.

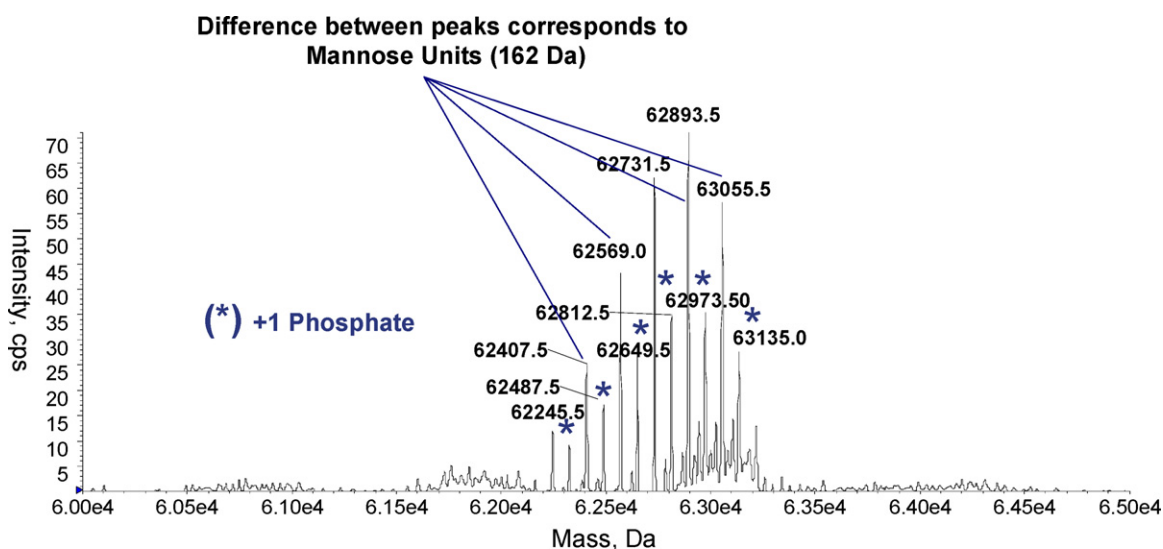
The highly acidic nature of native sulfonated glycans required analysis with normal-phase chromatography and negative-ion MS detection. The development of nanoflow chromatographic methods for acidic N-linked glycans has allowed for the very sensitive MS detection of underivatized carbohydrates and this approach was applied to the analysis of sialylated N-linked glycans that are also sulfonated [17]. For the work presented here, an aliquot of the aqueous glycan solution was combined with acetonitrile and injected onto the nanoflow-chip system (Agilent Technologies, Inc.) with a nanocolumn (75 µm × 150 mm) containing an

amide-80 HILIC stationary phase (Tosoh, Corp.). Zaia et al. [18] previously described this method for glycosaminoglycan analysis. LC–MS analysis of sulfonated glycans was performed by separation with the nanoflow-chip system using gradient elution (80–24% acetonitrile over 60 min) and infused into an Agilent Q-TOF 6520 mass spectrometer at 400 nL/min. Analytical scale analysis was also performed with larger amounts of material utilizing HILIC separation (2.1 mm × 150 mm Amide 80, Tosoh, Corp.) and negative-ion detection on a linear ion-trap instrument (LTQ-XL, Thermo Scientific). Negative-ion mode MS analysis was performed over an *m/z* range of 50–3000 and further characterization of select ions was performed by CID fragmentation analysis.

3. Results and discussions

3.1. Global structural characterization of glycans: intact protein analysis

Velaglugerace alfa is a glycosylated lysosomal enzyme produced in a human cell line. This enzyme has five consensus sequences for N-linked glycosylation, of which the first four are fully glycosylated. The X-ray crystal structure shows the fifth site as buried within the molecule and fully unoccupied [19]. Additives to the cell-production medium produce a glycoprotein containing high-mannose type glycoforms of varying chain length, some of which



| Carbohydrate Composition | Theoretical Mass | Observed Mass | Difference (Da) | Error (ppm) |
|--------------------------|------------------|---------------|-----------------|-------------|
| (Man) 36 (GlcNAc) 8 | 63054 | 63055 | 1 | 16 |
| (Man) 35 (GlcNAc) 8 | 62892 | 62893 | 1 | 16 |
| (Man) 34 (GlcNAc) 8 | 62730 | 62731 | 1 | 16 |
| (Man) 33 (GlcNAc) 8 | 62568 | 62569 | 1 | 16 |
| (Man) 32 (GlcNAc) 8 | 62406 | 62407 | 1 | 16 |
| (Man) 30 (GlcNAc) 8 | 62244 | 62245 | 1 | 16 |
| (Man) 36 (GlcNAc) 8 P1 | 63134 | 63135 | 1 | 16 |
| (Man) 35 (GlcNAc) 8 P1 | 62972 | 62973 | 1 | 16 |
| (Man) 34 (GlcNAc) 8 P1 | 62810 | 62812 | 2 | 32 |
| (Man) 33 (GlcNAc) 8 P1 | 62648 | 62649 | 1 | 16 |
| (Man) 32 (GlcNAc) 8 P1 | 62486 | 62487 | 1 | 16 |
| (Man) 30 (GlcNAc) 8 P1 | 62244 | 62245 | 1 | 16 |

Fig. 1. LC–MS mass measurement of the intact velaglugerace alfa therapeutic glycoprotein showing the high-mannose and phosphorylated high-mannose glycoforms.

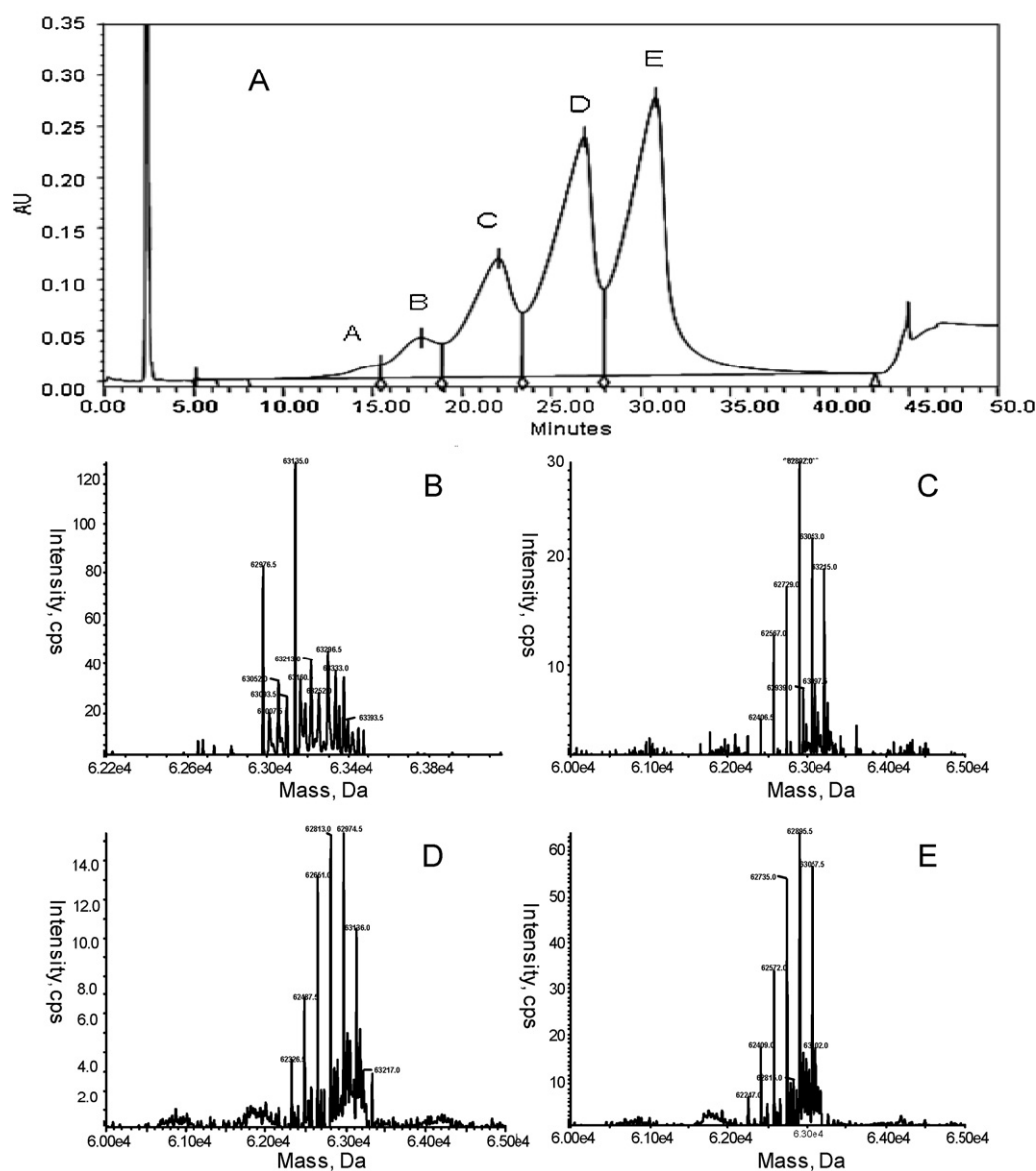


Fig. 2. LC–MS mass measurement from collected cation-exchange fractions. The results confirm that the charged species (peaks B–E) observed in the cation-exchange chromatogram are the result of phosphorylation at 0–4 glycosylation sites.

contain a single mannose-6-phosphate (M6P) unit. Heterogeneity exists in the types of glycans present as well as the site-specific variation in mannose units. Early mass-spectrometric measurements of intact glycoproteins have demonstrated the potential for characterization of their global glycan variation; however, limited information was previously obtainable for large heterogeneous glycoproteins due to the limitations in mass accuracy and resolution of early mass spectrometers [20]. The high resolution and mass accuracy offered by modern quadrupole time-of-flight (qTOF) mass spectrometers has made it possible to elucidate structural information at the intact protein level for larger glycoproteins with complicated glycan heterogeneity. With an instrument resolution of 10,000 FWHM and a mass accuracy of approximately 20 ppm using external calibration, mass differences greater than 20 Da are readily discernible for velaglycerase α . Comparing the observed masses to the theoretical value, the mass of each observed component has on average a mass error of 20 ppm. The deconvoluted spectrum demonstrates a series of neutral masses that correspond to changes of individual mannose and phosphate units (Fig. 1). For example, the observed molecular mass of velaglycerase with

(Man)₃₆(GlcNAc)₈ was 63,055 Da, which is a difference of 1 Da (16 ppm) when compared to the theoretical value of 63,054 Da. The accuracy is sufficient to make a positive identification of many of the heterogeneous components on intact velaglycerase α .

The same mass-spectral approach was used to characterize the peaks observed with weak cation-exchange (WCX) chromatography (Fig. 2A). In WCX separation, more acidic or negatively charged species elute prior to neutral and more basic or positively charged species. For peaks A–E, fractions were collected from the weak cation-exchange column and subjected to LC–MS analysis. Deconvoluted mass spectra for fractions B, C, D, and E are shown in Fig. 2B, C, D and E, respectively. Fraction A was less than 2% of total peak area and did not provide sufficient signal intensity to identify the glycoforms associated with this peak. Fractions corresponding to the remaining WCX peaks contain decreasing levels of phosphorylated species going from peak B to peak E, which is also in order of retention time. This finding is consistent with the expected elution order of the negatively charged phosphate species when separated by cation-exchange chromatography.

Accurate mass measurements of fractionated velaglucerase alfa by LC–MS analysis confirm that the charged species associated with peaks B–E in the WCX chromatogram are the result of 0–3 phosphorylation events with the earlier eluting peak B having 3 phosphates and the later eluting peak E having no phosphate. For each fraction, the WCX re-injection profile as well as analysis by isoelectric focusing provides further support for these identifications (data not shown). Even though the spectra for peak A were inconclusive, the glycoproteins in this peak are likely to have one phosphate more than the glycoproteins in peak B based on a retention time difference consistent with those seen between peaks B–E.

Since this global approach can only monitor the sum of all posttranslational modifications, this method cannot differentiate a single high-mannose type glycan with two phosphates from two high-mannose type glycans with a single phosphate each or a neutral glycan with an added mannose unit. Therefore, we take a more detailed approach to characterize and understand the individual glycan types.

3.2. Global structural characterization of glycans: total glycan release

MALDI-TOF MS analysis of permethylated glycans was used to establish the glycan profiles for velaglucerase alfa and agalsidase alfa. Fig. 3A shows velaglucerase alfa to have a simpler profile than agalsidase alfa (Fig. 3B). The cell culture process for velaglucerase

alfa is controlled to produce a predominance of high-mannose type glycans. Fig. 3A confirms the presence of the expected glycans.

The profile in Fig. 3B consists of a variety of glycan types that include high-mannose, hybrid, and complex glycans with the complex glycans having sialylation and core fucosylation (Table 1). Since the characterization of sialylated complex glycans is well established in the published literature, here we discuss the structural characterization of the phosphorylated glycans as well as their neutral counterparts. Table 2 summarizes the identified neutral and phosphorylated high-mannose glycans enclosed by the box shown in Fig. 3B. The observed masses are consistent with high-mannose glycans ranging from $\text{Man}_{5-7}\text{GlcNAc}_2$, phosphorylated high-mannose glycans ranging from $\text{Man}_{6-7}\text{GlcNAc}_2$, GlcNAc capped phosphate on the high-mannose glycan $\text{Man}_7\text{GlcNAc}_2$, and a hybrid glycan that is sialylated and phosphorylated. It is worth noting that the phosphate ester bond is stable during both the permethylation and ionization processes and was observed in the MALDI and ESI-MS spectra, which is consistent with other reports [21,22].

The structural assignments for phosphorylated high-mannose glycans were based on the ESI-MS/MS analysis of the permethylated $[\text{M}+2\text{Na}]^{2+}$ ions (Fig. 4). Challenges in assigning structures to phosphorylated glycans involve determination of the antenna structure that contains the phosphoester bond and whether this bond is on the terminal or an internal mannose unit. By comparing the MS/MS spectra for the neutral high-mannose glycans to the cor-

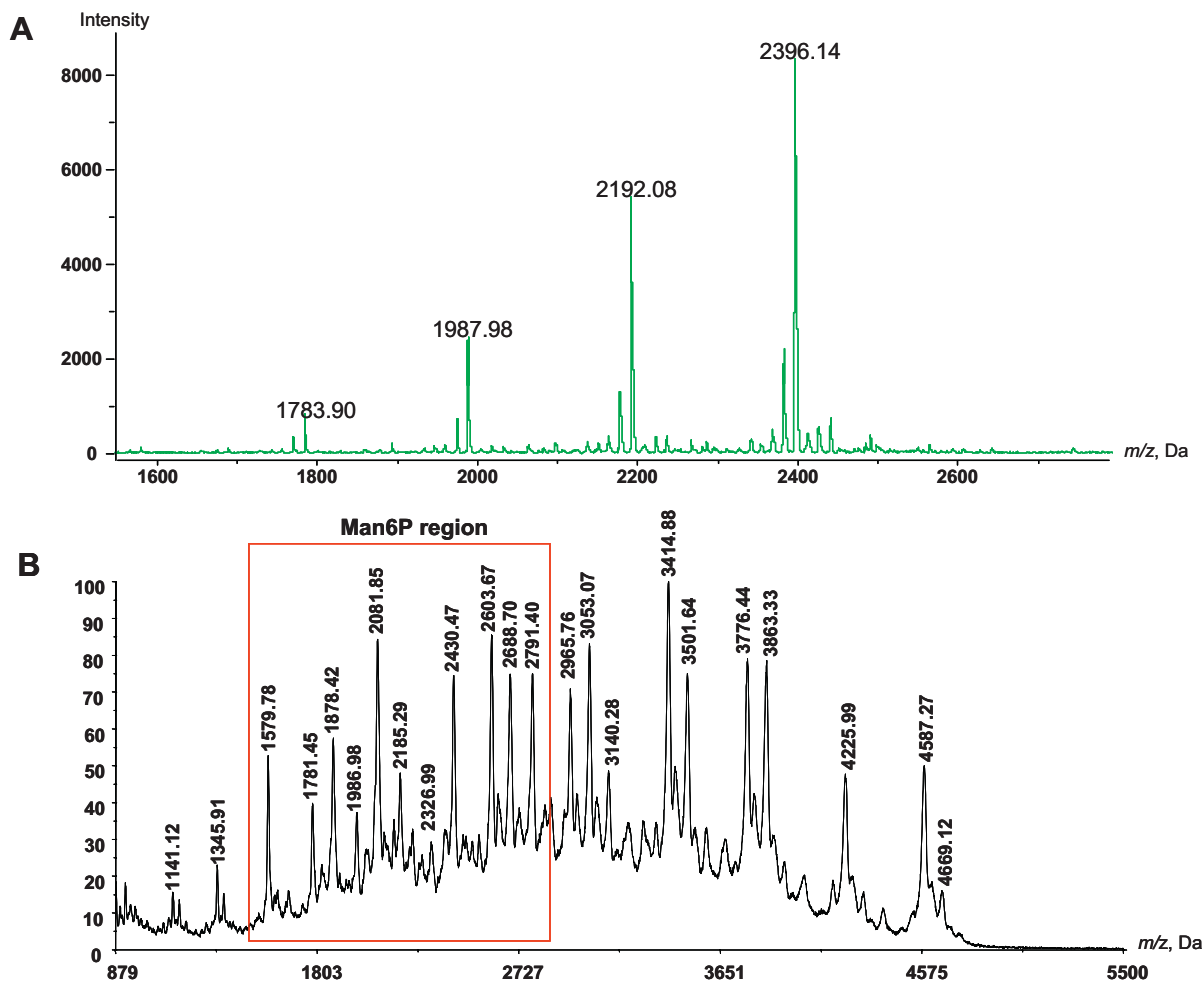


Fig. 3. The MALDI-TOF MS profile of sodiated permethylated glycans released from velaglucerase alfa (A) and agalsidase alfa (B). Panel A consists mainly of high-mannose glycans and panel B a heterogeneous mixture of high-mannose, hybrid, and complex glycans that are sialylated and core fucosylated. The box outlines the glycans containing M6P and their neutral counterparts. The spectrum in panel A was obtained using a Bruker Microflex System while panel B was obtained using a Voyager-DE MS.

Table 1

Compositional assignment for $[M+Na]^+$ glycans observed in the MALDI-TOF-MS spectra of agalsidase alfa [hexose = Hex, N-acetylhexosamine = HexNAc, phosphate = P, sialic acid = S, fucose = F].

| <i>m/z</i> obs | <i>m/z</i> calc | Composition | Glycan type |
|----------------|-----------------|---|---------------|
| 1345.91 | 1345.67 | Hex ₃ HexNAc ₂ F | High-man |
| 1579.78 | 1579.78 | Hex ₅ HexNAc ₂ | High-man |
| 1781.45 | 1783.88 | Hex ₆ HexNAc ₂ | High-man |
| 1878.42 | 1877.88 | Hex ₆ HexNAc ₂ P | High-man |
| 1986.98 | 1987.98 | Hex ₇ HexNAc ₂ | High-man |
| 2081.85 | 2082.97 | Hex ₇ HexNAc ₂ P | High-man |
| 2185.29 | 2186.08 | Hex ₅ HexNAc ₃ S | Hybrid |
| 2326.99 | 2328.07 | Hex ₇ HexNAc ₃ P | High-man |
| 2430.47 | 2431.21 | Hex ₅ HexNAc ₄ S | Complex/bi |
| 2603.67 | 2605.29 | Hex ₅ HexNAc ₄ FS | Complex/bi |
| 2688.70 | 2689.27 | Hex ₇ HexNAc ₃ PS | Hybrid |
| 2791.40 | 2792.38 | Hex ₅ HexNAc ₄ S ₂ | Complex/bi |
| 2965.76 | 2966.47 | Hex ₅ HexNAc ₄ S ₂ F | Complex/bi |
| 3053.07 | 3054.52 | Hex ₆ HexNAc ₅ FS | Complex/tri |
| 3140.28 | 3142.57 | Hex ₇ HexNAc ₆ F | Complex/tetra |
| 3414.88 | 3415.69 | Hex ₆ HexNAc ₅ FS ₂ | Complex/tri |
| 3501.64 | 3503.75 | Hex ₇ HexNAc ₆ FS | Complex/tetra |
| 3776.44 | 3776.87 | Hex ₆ HexNAc ₅ FS ₃ | Complex/tri |
| 3863.33 | 3864.92 | Hex ₇ HexNAc ₆ FS ₂ | Complex/tetra |
| 4225.99 | 4226.09 | Hex ₇ HexNAc ₆ FS ₃ | Complex/tetra |
| 4587.27 | 4587.27 | Hex ₇ HexNAc ₆ FS ₄ | Complex/tetra |

responding glycan containing a mannose-6-phosphate unit (M6P), assigning the location of the phosphoester bond becomes unequivocal. Branching assignments depend on cross-ring cleavages for key mannose units in the MS/MS spectra, which will define the specific high-mannose isomer for a given glycan. In the case of M6P, the cross-ring cleavages $^{0,4}A$ and $^{3,5}A$ suggest a location of the M6P on the 6-antennae of the core mannose unit, while the $^{2,4}A$ cleavage suggests linkage at the 3-antennae.

The MS/MS spectra of Man₇GlcNAc₂ show fragment ions representing glycosidic and cross-ring cleavages with fragment ion

assignments made according to Domon and Costello's nomenclature for glycans [23]. Three isomers (labeled 7A, 7B and 7C in Fig. 5) deduced from the ESI-MS/MS spectra of Man₇GlcNAc₂ (Fig. 4A) and the cross-ring cleavages that define them are tabulated in Fig. 5. Isomer 7A is distinguished by the presence of three mannoses at the 6-position of the core mannose, as demonstrated by the $^{0,4}A_4$ (*m/z* 709) and $^{3,5}A_4$ (*m/z* 737) ions. Moreover, the $^{2,4}A_4$ ion (*m/z* 723) suggests there are three mannoses at the 3-position of the core mannose. Isomer 7B can be differentiated from 7C by their $^{0,4}A_3$ ions, with 7B having *m/z* 301 compared to *m/z* 505 for 7C. Both also contain the $^{2,4}A_4$ ion (*m/z* 519) suggesting two mannose units at the 3-position of the core mannose.


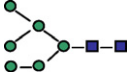



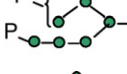
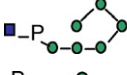

For the phosphorylated high-mannose glycans, similar fragment ions to that of the non-phosphorylated glycan are present in the spectra; however, there are distinct ions that indicate the presence of M6P. These characteristic ions are present in the spectra for both the monophosphorylated and diphosphorylated high-mannose glycans. The cross-ring cleavage ions $^{0,2}X_5$ and $^{1,5}X_5$ suggest that the phosphoester bond is located at the 6-position of the mannose. While the loss of C₂H₇PO₄ and C₃H₉PO₄ cannot identify the location of the phosphoester bond, these neutral losses are unique to phosphorylated glycans. As with the non-phosphorylated Man₇GlcNAc₂ glycan, three isomers are identified from similar cross-ring cleavage assignments for the corresponding phosphorylated glycan (Figs. 4B and 5).

3.3. Site-specific characterization of glycans

Identification and quantitation of glycopeptides is becoming a standard approach for assessing the site-specific glycosylation of therapeutic glycoproteins [24]. In the case of lysosomal enzymes, where cellular trafficking is dependent on phosphorylated high-mannose glycans [8,25,26], methods to compare phosphorylated and neutral glycans have potential to aid the development and

Table 2

The neutral and phosphorylated glycan structures for agalsidase alfa determined from the cross-ring cleavages observed in the MS/MS spectra of the released and perme-thylated glycans.

| <i>m/z</i> obs | <i>m/z</i> calc | Composition | Glycan structure |
|----------------|-----------------|---|---|
| 1579.78 | 1579.78 | Hex ₅ HexNAc ₂ |  |
| 1781.45 | 1783.88 | Hex ₆ HexNAc ₂ |  |
| 1878.42 | 1877.88 | Hex ₆ HexNAc ₂ P |  |
| 1986.98 | 1987.98 | Hex ₇ HexNAc ₂ |  |
| 2081.85 | 2082.97 | Hex ₇ HexNAc ₂ P |  |
| 2176.11 | 2177.96 | Hex ₇ HexNAc ₂ P ₂ |  |
| 2326.99 | 2328.07 | Hex ₇ HexNAc ₃ P |  |
| 2688.70 | 2689.27 | Hex ₇ HexNAc ₃ PS |  |

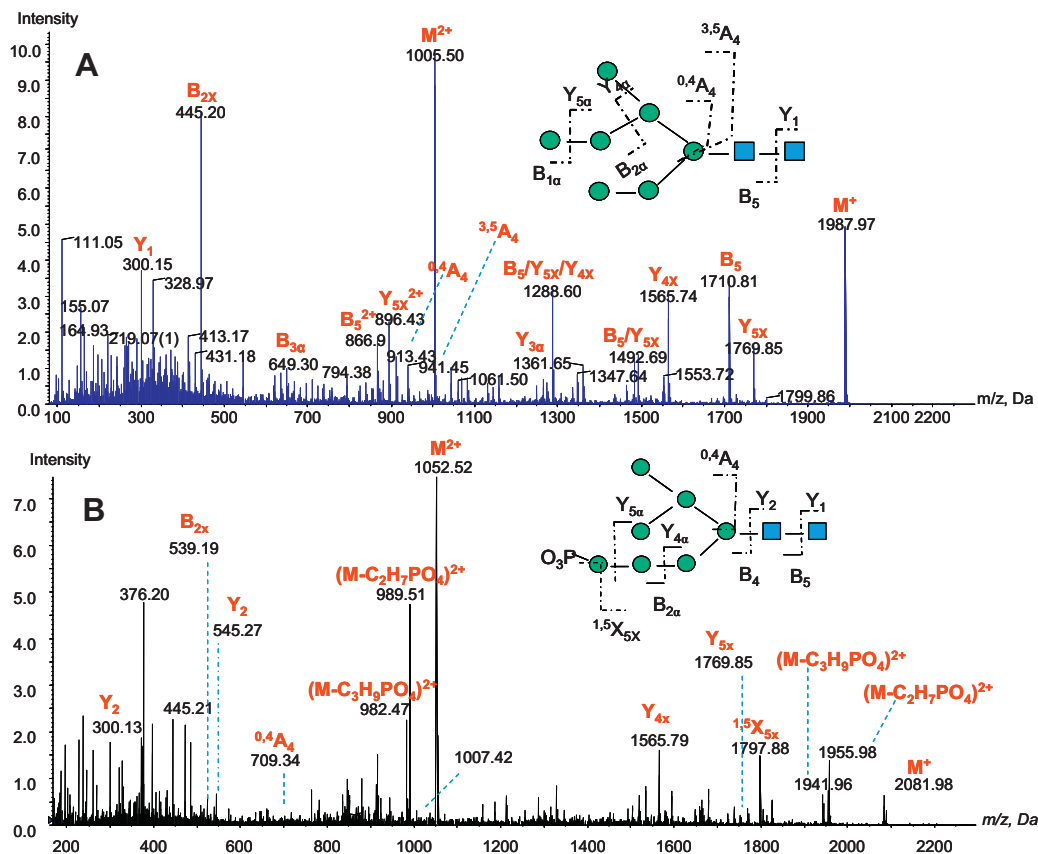
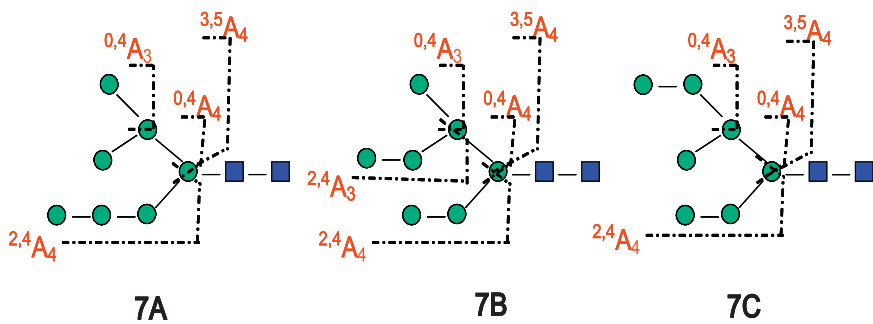


Fig. 4. The product ion spectrum of Man₇GlcNAc₂ (A) acquired from ESI-MS/MS analysis of the [M+2Na]²⁺ ion (m/z 1005.50). The structure (inset) deduced from the spectrum corresponds to isomer 7B. The MS/MS spectrum for the phosphorylated Man₇GlcNAc₂ (B) is indicative of the 7A isomer. Ions in each spectrum are labeled using nomenclature defined by Domon and Costello for glycosidic and cross-ring bond cleavages.



| Isomer | Observed Ions (m/z) | | | | | |
|--------|---------------------|-------------------|-------------------|-------------------|-------------------|-------------------|
| | 0,4A ₃ | 3,5A ₃ | 2,4A ₃ | 0,4A ₄ | 3,5A ₄ | 2,4A ₄ |
| 7A | 301 | -- | -- | 709 | 737 | 723 |
| 7B | 301 | -- | 519 | 913 | 941 | 519 |
| 7C | 505 | 533 | -- | 913 | 941 | 519 |

Fig. 5. The identity of cross-ring fragment ions from permethylated high-mannose glycans. The glycosidic bond and cross-ring cleavage patterns for the Man₇GlcNAc₂ glycan help to differentiate the structural isomers. The labeled cleavages are derived from the MS/MS fragmentation spectra.

manufacture of such therapeutic enzymes. Toward developing such a method, the glycan microheterogeneity at each site of glycosylation on agalsidase alfa was characterized using traditional peptide mapping methodologies coupled with LC–MS analysis. With this method, quantitation of the various glycoforms was possible using peak area analysis of the extracted ion chromatograms (EIC) for all glycans of interest. To verify the accuracy obtained with quantifying mass-spectral chromatograms, we compare values determined from the UV profile (214 nm), where signal detection comes primarily from the peptide backbone and with minimal UV absorption attributed to the glycan.

Fig. 6 contains the integrated chromatograms for a glycopeptide with multiple glycan species as well as for the peptide without a glycan (i.e., unoccupied peptide). The glycopeptide contains 24 amino acids, and has a variety of glycan types that also affect retention by reversed-phase chromatography. The glycan species consist of sialylated and neutral complex, sialylated and neutral hybrid, as well as neutral, mono-, and diphosphorylated high-mannose glycans. For a list of site-specific glycans (Asn184) observed on this agalsidase alfa glycopeptide, refer to Table S1 in the supplemental data.

To assess the quantitative effects of negatively charged glycans on ionization, the relative levels of each glycan type were compared by peak area analyses of the EIC, base peak, and TIC mass-spectral chromatograms, which were standardized to the same analysis of the UV chromatogram. Here we use the UV data as the accurate measurement since this analysis is based solely on the peptide backbone with no interference from the attached glycan.

The effect of negatively charged glycans on glycopeptide ionization during positive-ion mode analyses can influence quantitation due to uncertainty in the ionization potential from different glycoforms. Table 3 lists the peak areas, their percent of the total area for each chromatogram, and the percent deviation from the levels determined for the UV chromatogram. These results demonstrate that sialylated species have a negative percent deviation when compared to values determined from the UV chromatogram, while phosphorylation imparts a positive change (i.e., increase in peak area). This opposite effect for sialylated versus phosphorylated glycans suggests that the glycan type impacts the quantitation of glycopeptides from mass-spectral chromatograms more than the amount of negative charge. Not surprisingly, the largest change

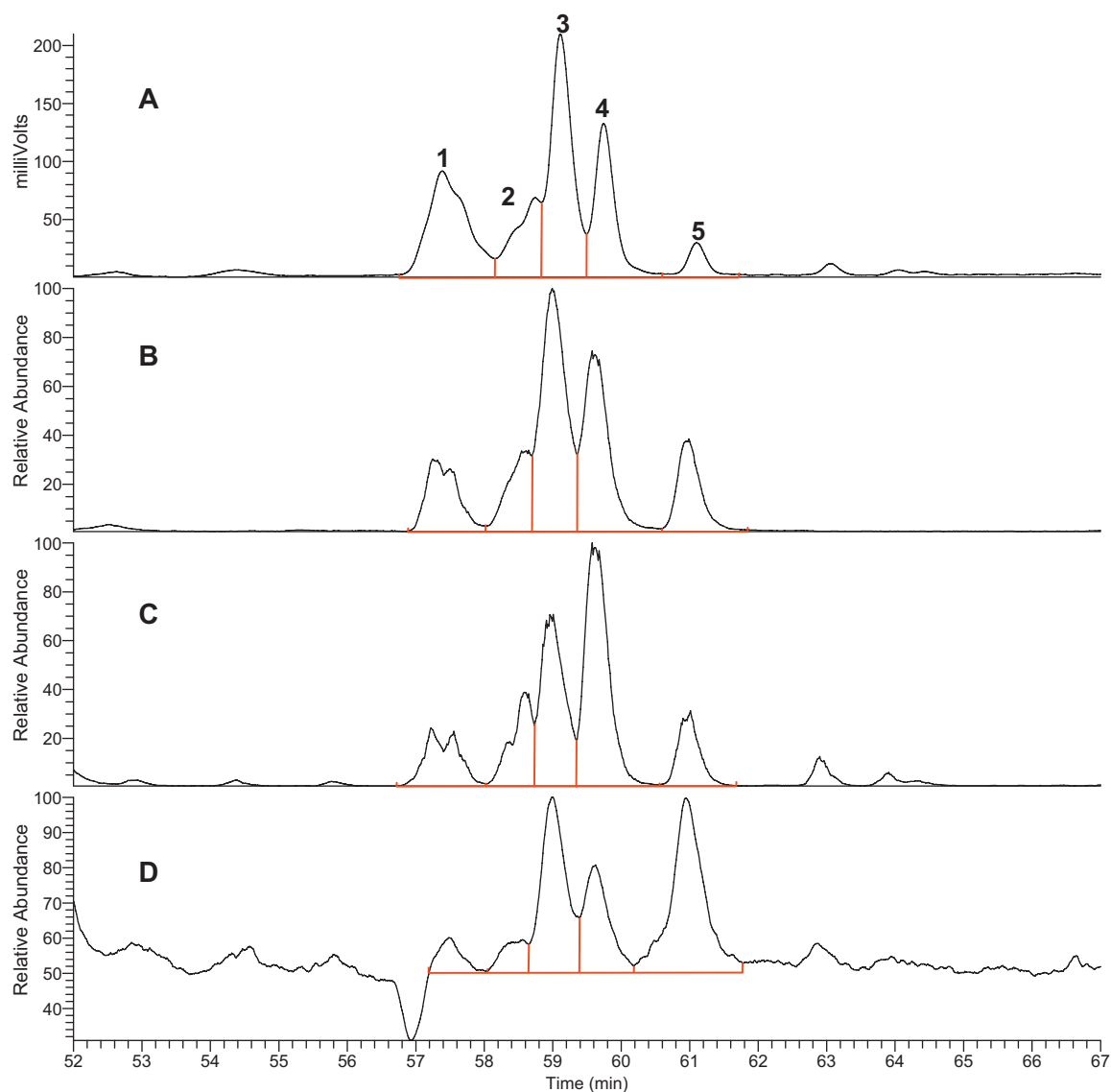


Fig. 6. Integrated chromatographic profiles for the Asn184 glycosylation site of agalsidase alfa used for the analysis shown in Table 3. The glycans consist of sialylated complex (peak 1), neutral complex, high-mannose and hybrid (peak 2), monophosphorylated hybrid and high-mannose (peak 3), diphosphorylated high-mannose (peak 4), and unoccupied peptide (peak 5). The four profiles correspond to various detection methods: UV absorbance at 214 nm (A), EIC using 20 m/z values corresponding to observed glycopeptides and the unoccupied peptide (B), the base peak chromatogram (C), and TIC (D). Red lines indicate the integration pattern.

Table 3

Glycopeptide peak area analysis from UV and mass spectral chromatograms demonstrates the inaccuracy of MS quantitation for the Asn184 site of agalsidase alfa.

| Chromatogram type | Glycan type | Peak area | Percent total peak area | Percent deviation from UV values |
|--------------------------|--|------------|-------------------------|----------------------------------|
| UV absorbance (214 nm) | Sialylated complex | 3468 | 27 | – |
| | Neutral complex, hybrid, and high-mannose | 1650 | 13 | – |
| | Monophosphorylated hybrid and high-mannose | 4629 | 36 | – |
| | Diphosphorylated high-mannose | 2577 | 20 | – |
| | Unoccupied | 468 | 4 | – |
| EIC | Sialylated complex | 9,172,679 | 13 | –51 |
| | Neutral complex, hybrid, and high-mannose | 7,474,853 | 11 | –16 |
| | Monophosphorylated hybrid and high-mannose | 24,852,894 | 36 | 0 |
| | Diphosphorylated high-mannose | 18,581,628 | 27 | 34 |
| | Unoccupied | 8,547,756 | 12 | 240 |
| Base peak (m/z 600–2000) | Sialylated complex | 4,671,294 | 12 | –55 |
| | Neutral complex, hybrid, and high-mannose | 4,855,290 | 13 | –3 |
| | Monophosphorylated hybrid and high-mannose | 10,392,043 | 27 | –26 |
| | Diphosphorylated high-mannose | 1,480,3061 | 38 | 90 |
| | Unoccupied | 3,943,787 | 10 | 179 |
| TIC | | | | |
| Not determined | | | | |

between mass spectral and UV derived values comes from the percent peak areas determined for the unoccupied peptide.

As with glycan type, the choice of mass-spectral chromatogram can also affect quantitation. The base peak and extracted ion chromatograms yield similar percent areas for the complex glycans. The percent peak areas, however, are different for the phosphorylated glycans, with base peak chromatograms yielding more than twice the percent deviation from the standard. Peak integration was not

performed for the TIC, since it was difficult to discern the complex and neutral peaks from the background noise.

Alkaline phosphatase treatment removes phosphate from terminal mannose but is inefficient at removing phosphate from internal mannose [27,28], which was evident with our exoglycosidase treatment studies (data not shown). In addition, alkaline phosphatase treatment alone does not distinguish phosphorylation on the glycan versus the peptide backbone. Therefore,

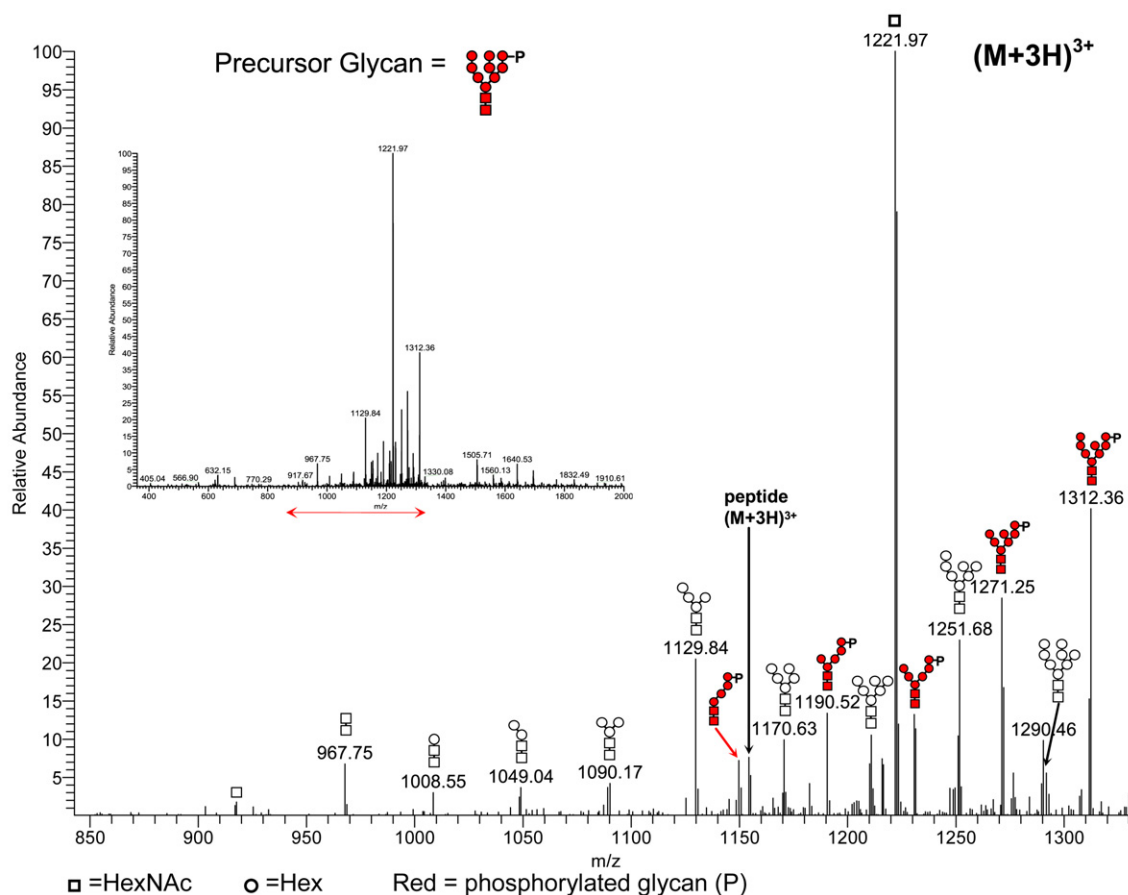


Fig. 7. The MS/MS spectrum for the velaglycerase alfa Asn270 glycopeptide (m/z 1352.55) with $(\text{Phos})_1(\text{Man})_9(\text{GlcNAc})_2$ verifies the presence of phosphate. The inset shows the entire m/z range with red arrows indicating the area shown in the detailed view. Fragment ion labels correspond to proposed monosaccharide compositions and do not include the peptide portion of the glycopeptide. The observed fragments suggest a high-mannose glycan with one phosphate at a terminal mannose as evident by the absence of the $(\text{Phos})_1(\text{Man})_3(\text{GlcNAc})_2$ glycan. (For interpretation of the references to color in this figure caption, the reader is referred to the web version of the article.)

demonstrating the presence of phosphate as well as its location on the glycan required LC-MS/MS fragmentation analysis of the proteolytically generated glycopeptide [29].

Analysis of the glycopeptide containing phosphate (Fig. 7) reveals a series of fragment ions that are unique to a phosphorylated $(\text{Man})_9(\text{GlcNAc})_2$. The fragmentation pattern demonstrates the susceptibility of the glycan group to fragmentation while providing protection to the peptide backbone. These fragment ions were consistent with the sequential cleavage of glycosidic bonds starting at the non-reducing end and terminating with the intact peptide. Observed in the MS/MS spectra were fragments containing a single M6P and 4–8 mannose units $[(\text{Phos})_1(\text{Man})_{4-8}(\text{GlcNAc})_2]$. Smaller fragments starting with $(\text{Man})_3(\text{GlcNAc})_2$ did not contain M6P, suggesting that the phosphate is located on the penultimate or terminal mannose. In addition, the MS/MS spectra for all the high-mannose glycans containing 7–9 mannose units and a single phosphate contain a glycan fragment ion (m/z 770) that is consistent with $(\text{Phos})_1(\text{Man})_3(\text{GlcNAc})_1$. At all four glycosylation sites, there was no evidence of $(\text{Phos})_1(\text{Man})_3(\text{GlcNAc})_2$ that would indicate phosphorylation close to or on the core mannoses. Together, the glycopeptide MS/MS fragmentation spectra are consistent with the presence of phosphate on a terminal mannose unit as previously discussed for the MS/MS fragmentation analysis of released permethylated glycans.

A series of fragment ions consistent with a glycan with and without phosphate were also observed in the MS/MS spectra, further demonstrating a single phosphorylation event (i.e., a difference of 80 Da). The observation of the two series of fragment ions from the same precursor, one with and one without phosphate, reveals differences in the phosphate's susceptibility to fragmentation, which suggests multiple sites of phosphorylation. Additionally, phosphate was not present on the smaller glycan fragments or the peptide without carbohydrate, confirming the identity of a phosphorylated glycan and not a phosphopeptide. Also consistent with the presence of a phosphorylated glycan, is the analysis of the peptide map after

PNGase F treatment, where there was no evidence of a neutral mass addition of 80 Da on the peptide (data not shown). In contrast, the MS/MS fragmentation analysis of the glycopeptide without phosphate reveals a similar series of fragment ions as those shown in Fig. 7 minus the phosphorylated fragments annotated in red.

Similar to the phosphorylated glycans, MS/MS analysis was used to verify the composition of complex glycans on glycopeptides. The fragmentation pattern for a trisialylated triantennary glycan with core fucosylation (refer to supplemental data Fig. S1) shows that the glycan protects the peptide from fragmentation and reveals marker ions (m/z 657) that are indicative of complex glycans. Fragments from this type of complex glycopeptide are observed from cleavage at the antennae, sialic acids and as with the phosphorylated glycans, glycosidic bonds.

Upon characterization of the site-specific glycans of idursulfase, we also observed an 80 Da addition to sialylated complex N-linked glycans on several glycopeptides, which suggested the presence of sulfonation. The unique properties of sulfonated glycans present additional challenges for mass-spectrometric analyses. Unlike phosphorylated glycans, sulfate moieties are not amenable to permethylation and incur potential losses during the permethylation procedure. Additionally, chromatographic methods for permethylated glycans have been limited to graphitized carbon columns where additional sample loss is known to occur [30]. Despite these challenges, recent reports have demonstrated the utility of MALDI-MS analysis of permethylated glycans containing sulfate [31,32]. In the work presented here, enrichment of sulfonated N-linked glycans was achieved by collecting late-eluting fractions from a strong anion-exchange column (refer to supplemental data Fig. S2). In order to characterize low levels of sulfonated glycans within a heterogeneous mixture of glycans from idursulfase, a HILIC-MS method was developed to analyze native sulfonated complex N-linked glycans.

The low levels of sulfonated glycans obtained from one of the glycosylation sites of idursulfase necessitated the use of nanoflow-

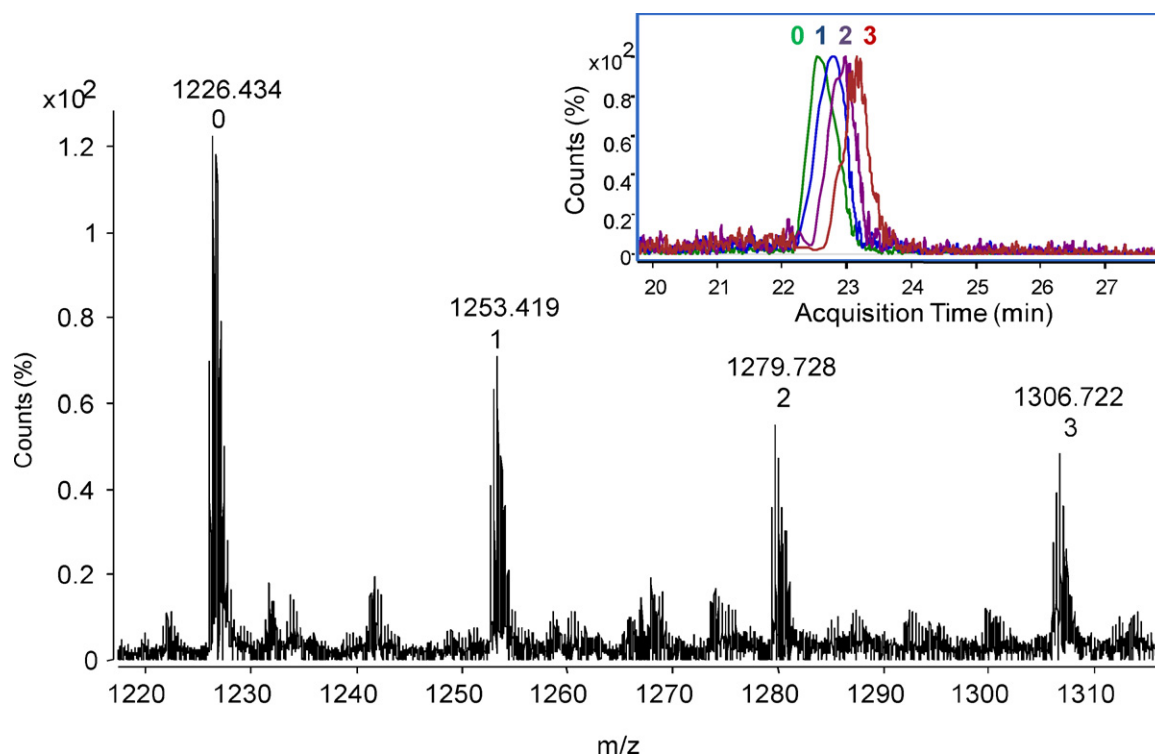


Fig. 8. Averaged HILIC-MS mass spectra for site-specific idursulfase sulfonated N-linked glycans. The triply-charged $(M-3H)^{3-}$ mass spectral peaks obtained in negative ion mode correlate to underivatized tetrasialylated N-linked glycans with 0–3 sulfates for the corresponding increases in m/z . EIC for the released glycans (inset) show the corresponding increase in elution time based upon sulfate number.

chip technology using a HILIC stationary-phase, which provides improved separation of the negatively charged sulfonated glycans. Coupled with efficient ionization and low sample consumption through nanoelectrospray technology, the nanoflow-chip allows for a sensitive and selective means to characterize low levels of sulfonated glycans. With the enhanced selectivity of this approach, 0–3 sulfates were observed on a tetrasialylated tetraantennary glycan (Fig. 8). Partial separation based upon sulfate number was achieved through the strong hydrophilic interaction of each sulfate moiety with the HILIC stationary phase. The elution order corresponds to an increasing number of sulfates where peak 0 represents the non-sulfonated glycan and peaks 1, 2 and 3 represent the mono-, di-, and trisulfonated glycans. Non-sulfonated glycans with varying levels of sialylation are separated and elute earlier than the sulfonated glycans (data not shown); however, sialylation of the sulfonated glycans has little effect on their separation. Phosphorylated high-mannose N-linked glycans also elute slightly earlier than sulfonated complex glycans. These observations show that retention on the HILIC column is stronger for the sulfonated species than the other acidic moieties.

The spectrum in Fig. 8 is obtained from a tetrasialylated tetraantennary glycan with core fucosylation with an average m/z of 1226.4. The observed monoisotopic mass of this species averaged over 20 full scans is 3681.295 ± 0.010 Da, which is comparable to the theoretical mass of 3681.297 Da for this species, representing a difference of 0.002 Da or a mass accuracy of -0.6 ppm. Additional evidence for the tetrasialylated tetraantennary structure in this work was obtained from sequential exoglycosidase treatment of

the corresponding site-specific glycopeptides followed by LC–MS analysis. The results show that four sialic acid residues are removed with sialidase treatment and subsequent removal of the four galactose residues occurs after removal of the sialic acid residues (data not shown). Synthesis of sialylated multiantennary N-linked glycans in mammalian cells is well-documented [33] and these results are consistent with those reports.

Small satellite peaks at intervals of approximately 27 m/z higher than the non-sulfonated glycan correspond to mono-, di-, and trisulfonated glycoforms [ca. m/z 1253.7, 1279.7, and 1306.7 as the $(M-3H)^{3-}$ charge, respectively]. The monoisotopic $(M-3H)^{3-}$ ion for the monosulfonated glycan, averaged over 26 full scans, was m/z 1252.742 ± 0.005 , which corresponds to a monoisotopic neutral mass of 3761.253 ± 0.015 Da. This mass is comparable to the theoretical monoisotopic mass of 3761.255 Da for a monosulfonated tetrasialylated tetraantennary fucosylated N-linked glycan with a mass error of -0.3 ppm (-0.001 Da). The next closest theoretical mass for the same complex glycan with a phosphate is 3761.263 Da, which has no precedence in the literature, and would have greater mass error (-2.1 ppm) when compared to the observed mass of the released glycan.

Additional evidence for the presence of sulfonated complex glycans was obtained by MS/MS fragmentation analysis of the monosulfonated species, which revealed several characteristic complex N-linked glycan fragments from the non-reducing end of this glycan but few internal fragments (Fig. 9A). The product ion spectrum was dominated by prominent losses of sialic acid (Y_7 ions) and loss of sulfate. The mass accuracy of the neutral 80 Da loss also

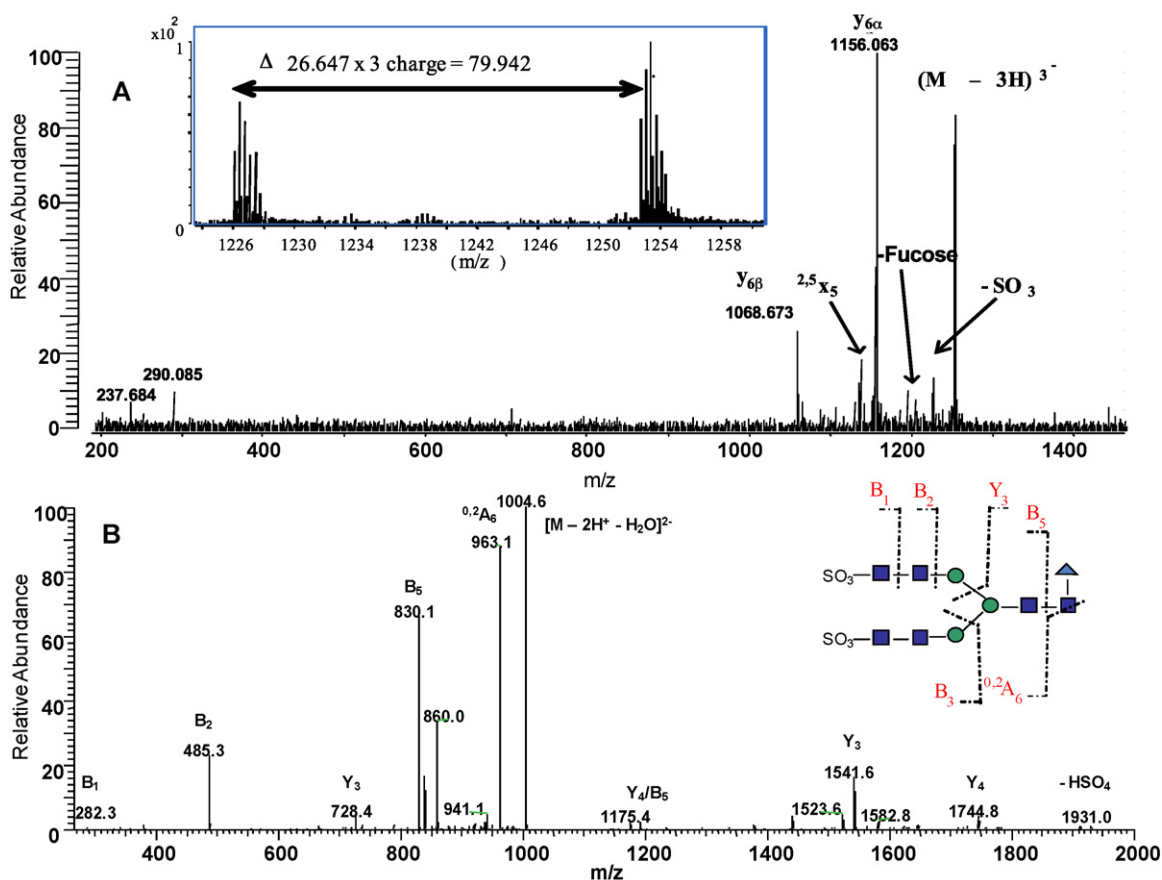


Fig. 9. HILIC–MS/MS fragmentation analysis of underivatized sulfonated complex glycans was used to locate the site of sulfonation. (A) The TOF product ion spectrum of a released sulfonated tetraantennary complex glycan from idursulfase. Four spectra were averaged to obtain accurate masses that are consistent with the loss of sulfate. The $(M-3H)^{3-}$ precursor ion targeted for MS/MS analysis shows prominent losses associated with sialic acid. The inset shows a calculated neutral mass loss consistent with the presence of sulfate. (B) The ion-trap product ion spectrum of released disulfonated N-linked glycans from bovine thyroid stimulating hormone. The $(M-2H)^{2-}$ precursor ion targeted for MS/MS analysis shows the sulfate located on the terminal GlcNAc.

supports a sulfate identity. Based upon the average of 4 MS/MS scans, the observed accurate mass difference for the sulfate loss was 79.942 ± 0.0277 Da. The theoretical mass for SO_3 is 79.957 Da while the theoretical mass for HPO_3 is 79.970 Da. This results in an observed neutral loss mass closer in value to the theoretical sulfate mass (a difference of -0.015 Da) than to a theoretical phosphate mass (a difference of -0.028 Da).

The HILIC–MS/MS methodology was evaluated for its capacity to provide structural information on underivatized sulfonated N-linked glycans. Sulfonated glycans on thyroid stimulating hormone (TSH) have been characterized by techniques including NMR and MALDI-MS [31,34,35] and shown to consist of asialo complex glycans with terminal sulfonation. These TSH glycans were easily obtainable from commercial sources and were used as model glycans for this study. TSH glycans were released from denatured bovine thyroid stimulating hormone (bTSH) and directly subjected to CID fragmentation.

The negative-ion MS/MS spectra of bTSH provided significant structural information (Fig. 9B) that aided the development of the HILIC–MS/MS method. The MS/MS fragmentation of the disulfonated biantennary glycan shows the location of one sulfate on the terminal end (i.e., the presence of a B fragment ion corresponding to HexNAc-SO_3^-) for each sulfonated antennae. However, MS/MS fragmentation analysis of the sulfonated tetrasialylated N-linked glycans of idursulfase reveals less structural information (Fig. 9A) for these glycans, despite applying a range of collision energies. Since the negative charge from both the sialic acid and sulfate moieties are readily lost upon CID, the facile loss of these charged groups reduces the amount of structural information obtainable with MS/MS fragmentation analysis.

Further structural analysis was performed on the sulfonated idursulfase glycans by exoglycosidase treatment of the sulfonated glycopeptides. Sequential treatments of the sulfonated glycopeptides with neuraminidase and β -galactosidase, followed by LC–MS analysis, showed that the sulfate moiety is not present on the terminal sialic acid or galactose residues (Gal-NeuAc). The resulting glycopeptides contained complex tetraantennary glycans terminating with HexNAc residues and retaining the sulfate (data not shown). Targeted RPLC–MS/MS analysis on desialylated sulfonated idursulfase glycopeptides provided additional evidence that the sulfate likely resides on the HexNAc residues of the antennae.

4. Conclusion

These results demonstrate the challenges of characterizing a heterogeneous glycan pool found on therapeutic glycoproteins, such as those used to treat lysosomal storage disorders. For enzyme replacement therapies, phosphorylated and sialylated N-linked glycans, as well as other glycoforms, provide critical attributes that define properties of the biotherapeutic and require thorough characterization. With the goal of producing well-characterized biologics, these studies demonstrate the utility of complementary mass-spectrometric methods in characterizing acidic glycans.

Global characterization of several therapeutic glycoproteins was obtained through two approaches: intact protein analysis and characterization of the total released glycans. The intact protein LC–MS analysis of velaglucerase demonstrated the distribution and range of phosphorylation on the high-mannose glycans. The same LC–MS approach was used to characterize the charge profile observed from ion-exchange analysis. The results showed a correlation between each ion-exchange peak and the addition of a phosphorylated glycan. MALDI- and electrospray-MS identification and structural characterization of the total released glycan pool was performed on velaglucerase alfa as well as agalsidase alfa. The results showed the presence of diphosphorylated high-mannose on agalsidase alfa,

while velaglucerase contained only monophosphorylated glycans. These results for velaglucerase alfa simplify the interpretation of the deconvoluted spectra for the intact protein, where the mass accuracy was not sufficient to distinguish between a diphosphorylated (160 Da) glycan from a species having an additional mannose unit (162 Da). Further structural analysis verified the site of the glycan phosphorylation to be on the 6-position of the mannoses.

Site-specific analysis of glycopeptides allowed for the identification and relative quantitation of phosphorylated and sialylated glycans. The results showed trends between UV quantitation of complex, phosphorylated high-mannose and neutral glycans compared to the relevant extracted ion chromatograms. Mono-phosphorylated and neutral glycan quantitation compared favorably to UV quantitation, whereas a decrease in the relative amounts of complex glycoforms and an increase in the relative amounts of diphosphorylated glycoforms were observed by mass spectrometry. The quantitative MS analysis of an unoccupied peptide fared worse than the UV quantitation. These results demonstrate the utility of the three MS quantitation approaches for the various glycoforms, with the extracted ion chromatograms being the better approach. However, this MS quantitation approach could not provide comparable results to those obtained with the standard UV chromatogram.

The presence of sulfonated N-linked glycans was confirmed through site-specific analysis of the released glycans of idursulfase. Their identification was revealed through accurate mass determination of the native glycans using HILIC–MS analysis. The results demonstrate the presence of up to three sulfate moieties on the fully sialylated tetraantennary complex glycans. While HILIC–MS/MS analysis of the model biantennary sulfonated glycans from bTSH demonstrated the methods ability to structurally characterize sulfonated glycans, improvements to sample preparation may be needed to elucidate the structures of sialylated and sulfonated complex glycans on idursulfase. However, additional characterization of the glycopeptides suggests that the sulfonation most likely exists on the N-acetylglucosamine residues, which is consistent with published reports for these types of glycans [32,36].

Acknowledgements

The authors thank Professor Joe Zaia and Dr. Gregory Staples for their helpful discussions and use of their chip-based LC–MS system. We also thank Eileen Golub and Sherry Castle for their LC–MS analysis of the peptide maps.

Appendix A. Supplementary data

Supplementary data associated with this article can be found, in the online version, at doi:10.1016/j.ijms.2011.06.017.

References

- [1] N. Jenkins, R.B. Parekh, D.C. James, *Nat. Biotechnol.* 14 (8) (1996) 975–981.
- [2] V. Kayser, N. Chennamsetty, V. Voynov, K. Forrer, B. Helk, B.L. Trout, *Biotechnol. J.* 6 (1) (2011) 38–44.
- [3] R.J.K. Sola, K. Griebenow, *BioDrugs* 24 (1) (2010) 9–21.
- [4] J.U. Baenziger, S. Kumar, R.M. Brodbeck, P.L. Smith, M.C. Beranek, *Proc. Natl. Acad. Sci. U.S.A.* 89 (1992) 334–338.
- [5] H. Masuda, Y. Takakura, M. Hashida, *Biochim. Biophys. Acta* 1426 (3) (1999) 420–428.
- [6] A. Varki, S. Kornfeld, *J. Biol. Chem.* 258 (5) (1983) 2808–2818.
- [7] T.S. Raju, J.B. Briggs, S.M. Chamow, M.E. Winkler, A.J. Jones, *Biochemistry* 40 (30) (2001) 8868–8876.
- [8] N.M. Dahms, L.J. Olson, J.J. Kim, *Glycobiology* 18 (9) (2008) 664–678.
- [9] A. Varki, S. Kornfeld, *J. Biol. Chem.* 255 (22) (1980) 10847–10858.
- [10] J.A. Cardelli, J.M. Bush, D. Ebert, H.H. Freeze, *J. Biol. Chem.* 265 (15) (1990) 8847–8853.
- [11] D. Fiete, V. Srivastava, O. Hindsgaul, J.U. Baenziger, *Cell* 67 (6) (1991) 1103–1110.

- [12] A.J. McVie-Wylie, K.L. Lee, H. Qiu, X. Jin, H. Do, R. Gotschall, B.L. Thurberg, C. Rogers, N. Raben, M. O'Callaghan, W. Canfield, L. Andrews, J.M. McPherson, R.J. Mattaliano, *Mol. Genet. Metab.* 94 (4) (2008) 448–455.
- [13] P.Y. Tong, W. Gregory, S. Kornfeld, *J. Biol. Chem.* 264 (14) (1989) 7962–7969.
- [14] V.S. Marjomaki, A. Salminen, *Basic Res. Cardiol.* 82 (3) (1987) 252–260.
- [15] S.A. Weston, C.R. Parish, *Eur. J. Immunol.* 22 (8) (1992) 1975–1981.
- [16] I. Ciucanu, F. Kerek, *Carbohydr. Res.* 131 (2) (1984) 209–217.
- [17] C.A. Cooper, E. Gasteiger, N.H. Packer, *Proteomics* 1 (2) (2001) 340–349.
- [18] G.O. Staples, H. Naimy, H. Yin, K. Kileen, K. Kraiczek, C.E. Costello, J. Zaia, *Anal. Chem.* 82 (2) (2010) 516–522.
- [19] B. Brumshtein, P. Salinas, B. Peterson, V. Chan, I. Silman, J.L. Sussman, P.J. Savickas, G.S. Robinson, A.H. Futerman, *Glycobiology* 20 (1) (2010) 24–32.
- [20] R.W. Oliver, B.N. Green, D.J. Harvey, *Biochem. Soc. Trans.* 24 (3) (1996) 917–927.
- [21] M.J.C. Miller, P.J. Savickas, Characterization of mannose-6-phosphate in lysosomal enzymes by tandem mass spectrometry, in: 55th ASMS Conference on Mass Spectrometry and Applied Topics, Indianapolis, IN, American Society for Mass Spectrometry and Applied Topics, 2007.
- [22] S. Sioud, F. Jahouh, M. Nashed, N. Joly, J.H. Banoub, *Rapid Commun. Mass Spectrom.* 24 (17) (2010) 2475–2490.
- [23] B. Domon, C.E. Costello, *Glycoconjugate J.* 5 (4) (1988) 397–409.
- [24] M.M. Ivancic, H.S. Gadgil, H.B. Halsail, M.J. Treuheit, *Anal. Biochem.* 400 (1) (2010) 25–32.
- [25] R.N. Bohnsack, X. Song, L.J. Olson, M. Kudo, R.R. Gotschall, W.M. Canfield, R.D. Cummings, D.F. Smith, N.M. Dahms, *J. Biol. Chem.* 284 (50) (2009) 35215–35226.
- [26] S. Kornfeld, *FASEB J.* 1 (6) (1987) 462–468.
- [27] V. Herzog, W. Neumuller, B. Holzmann, *EMBO J.* 6 (3) (1987) 555–560.
- [28] C. Isidoro, S. Grassel, F.M. Baccino, A. Hasilik, *Eur. J. Clin. Chem. Clin. Biochem.* 29 (3) (1991) 165–171.
- [29] H. Peltoniemi, S. Joenvaara, R. Renkonen, *Glycobiology* 19 (7) (2009) 707–714.
- [30] M. Pabst, F. Altman, *Anal. Chem.* 80 (19) (2008) 7534–7542.
- [31] M. Lei, Y. Mechref, M.V. Novotny, *J. Am. Soc. Mass Spectrom.* 20 (9) (2009) 1660–1671.
- [32] S.Y. Yu, S.W. Wu, H.H. Hsiao, K.H. Khoo, *Glycobiology* 19 (10) (2009) 1136–1149.
- [33] R. Kornfeld, S. Kornfeld, *Ann. Rev. Biochem.* 54 (1985) 631–664.
- [34] J. Hiyama, G. Weisshaar, A.G.C. Renwick, *Glycobiology* 2 (5) (1992) 401–409.
- [35] S.F. Wheeler, D.J. Harvey, *Anal. Biochem.* 296 (1) (2001) 92–100.
- [36] G.C. Gil, W.H. Velander, K.E. Van Cott, *Glycobiology* 18 (7) (2008) 526–539.